

# Ambiguity-Directed Sampling for Qualitative Analysis of Sparse Data from Spatially-Distributed Physical Systems

Chris Bailey-Kellogg

Dartmouth Computer Science Dept.  
6211 Sudikoff Laboratory  
Hanover, NH 03755  
cbk@cs.dartmouth.edu

Naren Ramakrishnan

Virginia Tech Dept. of Computer Science  
629 McBryde Hall  
Virginia Tech, VA 24061  
naren@cs.vt.edu

## Abstract

A number of important scientific and engineering applications, such as fluid dynamics simulation and aircraft design, require analysis of spatially-distributed data from expensive experiments and complex simulations. In such data-scarce applications, it is advantageous to use models of given sparse data to identify promising regions for additional data collection. This paper presents a principled mechanism for applying domain-specific knowledge to design focused sampling strategies. In particular, our approach uses ambiguities identified in a multi-level qualitative analysis of sparse data to guide iterative data collection. Two case studies demonstrate that this approach leads to highly effective sampling decisions that are also explainable in terms of problem structures and domain knowledge.

## 1 Introduction

A number of important scientific and engineering applications, such as fluid dynamics simulation and aircraft design, require qualitative analysis of spatially-distributed data from expensive experiments and/or complex simulations demanding days, weeks, or even years on petaflops-class computing systems. For example, Fig. 1 shows a cross-section of the design space for a multidisciplinary aircraft design problem involving 29 design variables with 68 constraints in a highly non-convex design space [Knill *et al.*, 1999]. Fully exploring such large, multi-dimensional datasets is prohibitively expensive. Instead, design engineers must identify qualitative *pockets* of the space that merit further consideration. Two important characteristics distinguish these applications: (1) data scarcity, due to the cost and time for data collection; and (2) complete control by the scientist or engineer over the data acquisition process (e.g. regions of the design space where data can be collected, especially via computer simulations). It is natural therefore to focus data collection so as to maximize information content, minimize the number and expense of samples, and so forth.

This paper presents a principled mechanism for applying domain-specific knowledge to focus sampling strategies for

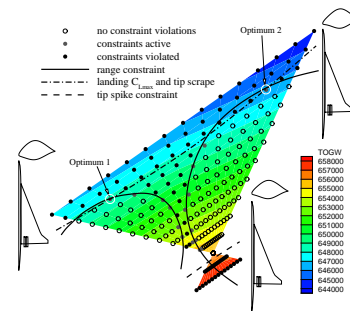


Figure 1: A pocket in an aircraft design space viewed as a slice through three design points (courtesy Layne T. Watson).

data-scarce applications. In particular, *ambiguities* identified by multi-level qualitative analysis of data collected in one iteration guide succeeding iterations of data collection so as to improve the qualitative analysis. This approach leads to highly effective sampling decisions that are *explainable* in terms of problem structures and domain knowledge. We demonstrate the effectiveness of our approach by two case studies: (1) identification of pockets in  $n$ -dimensional space, and (2) decomposition of a field based on control influences.

## 2 Qualitative Analysis of Spatially-Distributed Physical Systems

The mechanism we develop for ambiguity-directed sampling is based on the Spatial Aggregation Language (SAL) [Yip and Zhao, 1996; Bailey-Kellogg *et al.*, 1996], which supports construction of data interpretation and control design applications for spatially-distributed physical systems. SAL programs uncover and manipulate multi-layer geometric and topological structures in spatially distributed data by using a small number of uniform operators and data types, parameterized by domain-specific knowledge. These operators and data types mediate increasingly abstract descriptions of the input data, as shown in Fig. 2. They utilize knowledge of physical properties such as continuity and locality, based on specified metrics, adjacency relations, and equivalence predicates, to uncover regions of uniformity in spatially distributed data.

As an example (see Fig. 3), consider a SAL program for bundling the vectors in a given vector field (e.g. wind velocity or temperature gradient) into a set of streamlines (paths

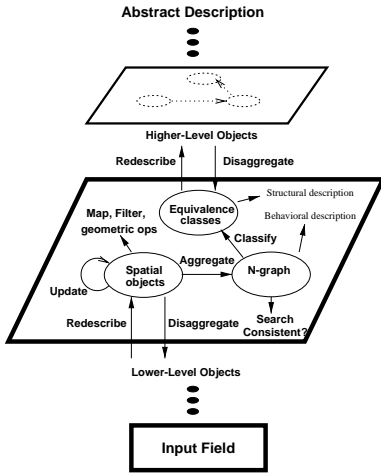


Figure 2: SAL multi-layer spatial aggregates, uncovered by a uniform vocabulary of operators utilizing domain knowledge.

through the field following the vector directions):

1. *Aggregate* vectors into a neighborhood graph (say 8-adjacency), localizing computation.
2. *Filter* edges in the graph, ensuring edge direction is similar enough to vector direction.
3. Cluster into *equivalence classes* neighboring vectors whose directions match best.
4. *Redescribe* equivalence classes of vectors into more abstract streamline curves.

In a second level of abstraction, streamlines are aggregated and classified into groups with similar flow behavior (Fig. 3(d)), *using the exact same operators but with different metrics*. As this example illustrates, SAL provides a vocabulary for expressing the knowledge required — distance metrics, similarity metrics, etc. — for uncovering multi-level structures in spatial data sets. It has been applied to applications ranging from decentralized control design [Bailey-Kellogg and Zhao, 1999] to analysis of diffusion-reaction morphogenesis [Ordóñez and Zhao, 2000].

### 3 Ambiguity-Directed Sampling

This section extends SAL for data-scarce, rather than data-rich, applications, adding the operators in Tab. 1 for iteratively sampling a field based on qualitative features of the current data set. We note that structures can either be found in the sparse data itself, or in a dense data set generated by fitting a *surrogate function* to the samples. The mechanism presented here works with both approaches; in either case, new sample locations are suggested based on ambiguities in the uncovered structures.

#### 3.1 Bottom-Up Detection of Ambiguity

The SAL equivalence class clustering mechanism exploits continuity, grouping neighboring objects that satisfy a domain-specific equivalence predicate (e.g. similar vector direction). At discontinuities, dissimilar neighboring objects are placed in separate classes. However, within a

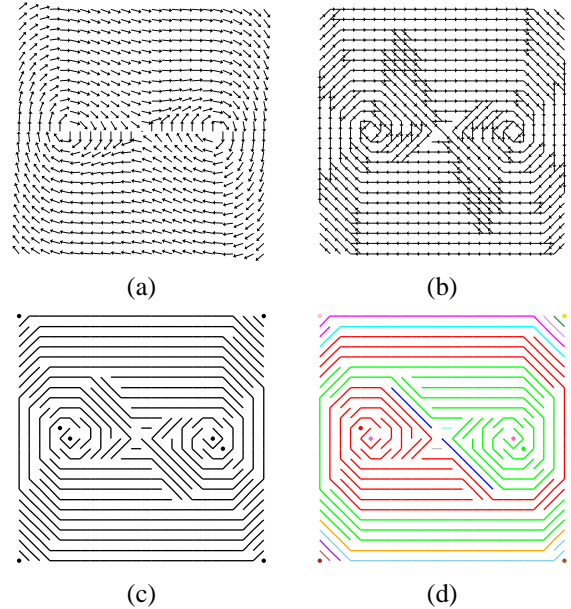


Figure 3: Example steps in SAL vector field analysis. (a) Input vector field. (b) Filtered neighborhood graph. (c) Equivalence classes (make a choice at each fork edge) redescribed as streamline curves. (d) Higher-level aggregation and classification of curves whose flows converge.

weakly-similar class or across a weakly-different discontinuity, neighboring objects might *almost* satisfy the predicate. For example, some vectors in Fig. 3(b) have two possible forward neighbors; in some cases, a vector might equally well belong to either of two flows. We call such unclear classification choice points *ambiguous*.

The bottom-up SAL operators previously introduced can thus be used to detect ambiguities if the equivalence class clustering mechanism is extended as in Tab. 1. In particular, a domain-specific equivalence predicate indicates when neighbors are equivalent, not equivalent, or ambiguous.

#### 3.2 Top-Down Utilization of Ambiguity

Ambiguity can reflect the desirability of acquiring data at or near the specified point, to clarify the correct classification and/or serve as a mathematical criterion of information content. Disambiguating between conflicting SAL interpretations can be posed as a model selection problem. Using SAL, we can compute a prior distribution on the conflicting models ( $\mathcal{P}(m)$ ) and use it to select a sample point  $s$  that maximizes an information-theoretic measure. This enables a two-stage iterative algorithm where newer data enable the selection of a model  $m$  that maximizes the posterior  $\mathcal{P}(m | s)$ , aiding qualitative analysis. The *sample* operator specified in Tab. 1 addresses this opportunity by generating samples to optimize a given domain-specific objective function over the set of ambiguous objects. For example, in response to a vector with an ambiguous neighbor, it might suggest nearby locations to sample. In other applications, it might pick the midpoint between a pair of ambiguous points, or even (see the influence-based model decomposition application below) apply SAL

<p><b>classify</b> : objects * equiv_predicate <math>\rightarrow</math> classes * ambiguous</p> <p>Apply predicate to neighboring objects, partitioning them into equivalence classes and left-over ambiguous objects. Predicate is a function taking a pair of neighbors and returning one of {true, false, ambiguous}.</p> <p><b>sample</b> : ambiguous * objective_function <math>\rightarrow</math> objects</p> <p>Determine new objects to be sampled based on optimization of an objective function over the set of ambiguous objects.</p>
--

Table 1: Ambiguity-directed sampling operators.

recursively to qualitatively analyze a set of ambiguous points.

Data are collected for the indicated sample points (by experiment or simulation). When a surrogate function is used, *sample* refines the fitted model at the indicated points with the real data. We note that efficient implementations of some data structures (e.g. Delaunay triangulation neighborhood graphs) can be incrementally updated with the additional samples [Ordóñez and Zhao, 2000]. The aggregation process can then be iterated with the improved data set, terminating when information-theoretic measures such as entropy and information gain reach specified levels.

## 4 Applications

This section discusses how the computational framework of two existing applications can be redescribed in terms of ambiguity-directed sampling, and then illustrates the effectiveness of our approach with two new case studies.

### 4.1 Existing Applications

KAM [Yip, 1991] interprets the behaviors of Hamiltonian dynamical systems by phase-space analysis. Geometric points represent states of the system for a given set of parameters. KAM groups points into orbits describing the system’s temporal evolution; it groups orbits into phase portraits describing evolution of all states for a given set of parameters; and it groups phase portraits into bifurcation maps describing variations in portraits due to variations in parameters. At each stage, KAM adds samples when it detects an inadequate description. In our vocabulary, the *classify* predicate clustering orbits into a phase portrait notices when two neighboring orbits cannot physically be adjacent; *sample* then starts orbit integration from the mid-point of an ambiguous pair of neighboring points. Similarly, in a bifurcation map additional phase portraits are generated for parameter values between those of ambiguous neighboring phase portraits.

STA [Ordóñez and Zhao, 2000] has been applied to build high-level descriptions of morphogenesis in diffusion-reaction systems by tracking aggregates of sample “floaters” that react to changes in the underlying field. In particular, in a manner similar to the particle system of Witkin and Heckbert [1994], floaters attempt to ensure an adequate sampling of the field, especially in high-gradient areas, by repelling each other, splitting, and merging. In our vocabulary, the *classify* predicate bundling floaters in a region tests whether or not neighboring floaters are near enough relative to an energy metric measuring adequate representation of the region; *sample* simply splits one ambiguous floater into two adjacent floaters.

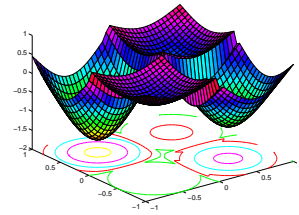


Figure 4: A 2D pocket function.

### 4.2 Pocket Identification

As discussed earlier, identification of pockets is important in engineering design. This case study validates our approach with a difficult-to-optimize pocket function, designed by de Boor (Fig. 4):

$$\begin{aligned} \alpha(\mathbf{X}) &= \cos \left( \sum_{i=1}^n 2^i \left( 1 + \frac{x_i}{|x_i|} \right) \right) - 2 \\ \delta(\mathbf{X}) &= \|\mathbf{X} - 0.5\mathbf{I}\| \\ p(\mathbf{X}) &= \alpha(\mathbf{X})(1 - \delta^2(\mathbf{X})(3 - 2\delta(\mathbf{X}))) + 1 \end{aligned}$$

where  $\mathbf{X}$  is the  $n$ -dimensional point  $(x_1, x_2, \dots, x_n)$  at which the pocket function  $p$  is evaluated,  $\mathbf{I}$  is the identity  $n$ -vector, and  $\|\cdot\|$  is the  $L_2$  norm.

This function exploits the counterintuitive fact that the volume of a high-dimensional cube is concentrated in its corners. There are  $2^n$  pockets (local minima), making naive global optimization infeasible. However, in real-world domains, significant structure exists and can often be exploited. A good example is the STAGE algorithm [Boyan and Moore, 2000] that intelligently selects starting points for local search algorithms. *Our goals here are very different from global optimization*: we wish to obtain a qualitative indication of the existence, number, and locations of pockets, using low-fidelity models and/or as few data points as possible. The results can then be used to seed higher-fidelity calculations. This is also fundamentally different from DACE [Sacks *et al.*, 1989], polynomial response surface approximations [Knill *et al.*, 1999], and other approaches in geo-statistics where the goal is accuracy of functional prediction at untested data points. Here, accuracy of estimation is traded for the ability to mine pockets.

In a dense field of data, it is straightforward to identify pockets by applying the vector field bundling implementation discussed in the introduction (see Fig. 3) to the gradient field. In the data-scarce setting, we adopt the following methodology: (1) generate a dense field by fitting a surrogate function to the current set of observations, (2) use SAL to identify pockets in the field, (3) use ambiguities in pocket identification to focus areas for future data collection, and (4) repeat. We adopt a sequential sampling strategy, which has the advantage of reducing the problem to a sequence of smaller optimizations, allowing the data mining to terminate when results of the desired fidelity are achieved. It also has the advantage of reacting at runtime to the determination of qualitative SAL structures.

The choice of surrogate representation is constrained by the local nature of SAL computations. In particular, a kriging-type interpolating estimator handles situations with multiple

**Vector equivalence predicate**

Return true if vector directions are similar enough, false if they aren't, and ambiguous if a vector has multiple neighbors with similar-enough directions.

**Sample objective function**

Minimize the entropy  $E(-\log d)$ , where  $d$  is the conditional density of  $p$  over the design space *not* covered by the current data values.

Table 2: Domain knowledge for ambiguity-directed sampling in pocket identification.

local extrema (weather maps, remote sensing, etc.) and can easily exploit anisotropies and trends. Given  $k$  observations of the pocket function, the model gives exact responses at these  $k$  sites and estimates values at other sites by minimizing the mean squared error (MSE), assuming a random data process  $Z$  with zero mean and a known covariance function. Formally, the estimated model (for two dimensions) is:

$$p'(x_i, y_i) = E(p(x_i, y_i) | p(x_1, y_1), \dots, p(x_k, y_k))$$

The true function  $p$  is assumed to be the realization of a random process such as:

$$p(x, y) = \beta + Z(x, y)$$

where  $\beta$  is typically a uniform random variate (estimated based on the known  $k$  values of  $p$ ).  $Z$  is usually expressed in terms of correlation functions and/or correlation matrices that could encode domain-specific constraints or reflect the current fidelity of data. The estimator for minimizing MSE is obtained by multi-dimensional optimization:

$$\max_C \left( \frac{-k}{2} \right) (\ln(\sigma^2) + \ln(|R|))$$

where  $R$  is the symmetric-correlation matrix of  $Z$  and  $\sigma^2$  is the *estimated* variance, both derived from and dependent on a predefined set of correlation parameters  $C$  (e.g., parameters that describe a product of uni-dimensional correlations).

Identification and exploitation of ambiguities uses the domain-specific knowledge summarized in Tab. 2. We fold the identified ambiguities into the kriging estimator by an approach reminiscent of incorporating 'Type C' soft data into variograms [Journel, 1986]. The basic idea is to use the distribution of ambiguous streamlines originating at a location as an indicator covariance term in the parameterization of  $Z$  (and by definition, in  $R$ ). By weighting the data values at different locations by the pdf of this 'ambiguity distribution,' we provide a novel mechanism to include qualitative information. Streamlines that 'agree' will generally contribute less to data mining, just as two samples close together will not contribute as much information as off-diagonal entries in the  $R$  matrix. Thus, this framework can be viewed as a natural generalization of the assumptions of sample clustering that underlie kriging.

We applied the ambiguity-driven mechanism to determining pockets in both 2D and 3D (the extension to higher dimensions is straightforward and is not described here for ease of presentation). We used a variation of the pocket function with a pseudorandom perturbation that shifts the

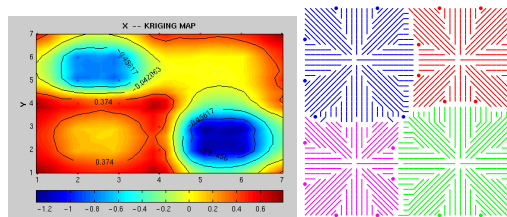


Figure 5: (left) Computed variogram from a design involving only 7 points. Isocontours of (estimated) MSE are also shown. Notice that the focused design completely skips one of the quadrants, a result hard to achieve without qualitative feedback. (right) SAL output from surrogate model data confirming the existence of four pockets.

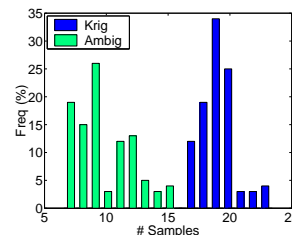


Figure 6: Pocket-finding results (2D) show that ambiguity-directed sampling always requires fewer samples than conventional kriging.

pockets away from the corners in a somewhat unpredictable way [Rice, 1992]. This twist precludes many forms of analyses, such as symbolic parsing, by imposing a highly nonlinear global map of pocket locations. The initial experimental configuration used a face-centered design (4 points in the 2D case). The surrogate model then generated a  $41^n$ -point grid. The ambiguity-directed mechanism selected new design points, using the vector field bundling approach discussed above. Standard parameter settings were applied: required similarity of 0.8 for dot product of adjacency direction and vector field direction, and factor of  $0.01 \cdot \text{distance}$  penalizing the grouping of far-apart vectors.

Fig. 5 shows the computed variogram and SAL pocket classification for a design computed from only 7 total data points. As previously discussed, our sampling decisions result in highly sub-optimal designs according to traditional metrics of variance in predicted values and D-optimality, but are sufficient to determine pockets. Fig. 6 shows the distributions of number of design points required for ambiguity-directed and kriging-based pocket identification over 100 perturbed variations of the 2D pocket function. Ambiguity-directed sampling required 3 to 11 additional samples, with the latter figure in the pathological case where the random perturbations cause a nearly quintic dip, rendering the initial adjacency calculations misleading. In comparison, conventional incremental kriging techniques required 13 to 19 additional data points. While pockets in the bigger dips are discovered quickly, the quintic and shallow dips require more function evaluations. Tests with pockets in 3D yielded even more significant results: up to 151 additional points for regular kriging, but at most 42 for ambiguity-directed sampling.

With the use of block kriging, reductions in both values could be enjoyed, but these figures illustrate the effectiveness of our technique.

### 4.3 Influence-Based Model Decomposition

*Influence-based model decomposition* [Bailey-Kellogg and Zhao, 1999] is an approach to designing spatially-distributed data interpretation and decentralized control applications, such as thermal regulation for semiconductor wafer processing and noise control in photocopy machines. A decentralized *influence graph*, built by sampling the effects of controls on a field (either physically or by solving a partial differential equation), represents influences of controls on distributed physical fields. Given the expense of obtaining influence graph values, it is desirable to minimize the number of samples required. This section demonstrates that ambiguity-directed sampling can greatly reduce the number of samples required. Note that we do not follow the explicit kriging methodology of the pocket application, since it sometimes does not result in explainable designs, by overlooking ‘nice’ properties such as balance, symmetry, collapsibility, and comparability.

Influence-based model decomposition uses influence graphs for control placement and parameter design algorithms that exploit physical knowledge of locality, linear superposability, and continuity for distributed systems with large numbers of coupled variables (often modeled by partial differential equations). By leveraging the physical knowledge encapsulated in influence graphs, these control design algorithms are more efficient than standard techniques, and produce designs explainable in terms of problem structures. Influence-based model decomposition decomposes a problem domain so as to allow relatively independent design of controls for the resulting regions. Fig. 7 overviews the approach:

1. Represent in an influence graph the effects of a few sample *probe* controls on the field — in this example, the heat flows induced in a piece of material by point heat sources.
2. Cluster the probes based on similarities in their effects, as represented in the influence graph. For example, the geometric constraint imposed by the narrow channel in the dumbbell-shaped piece of material results in similar field responses to the two probes in the left half of the dumbbell and similar responses to the two probes in the right half of the dumbbell. Note that influence graphs encapsulate not only geometry but also material properties, which can greatly impact heat flows and thus the proper decomposition.
3. Cluster the field nodes based on the probe clustering, applying a predicate testing if neighboring field nodes are well-represented by the same probe nodes. In the example, the field nodes in the left half of the dumbbell are best represented by the probe nodes also in the left half (which belong to the same probe equivalence class), and are thus decomposed from the nodes in the right half. Controls are placed in the regions and optimized by a separate process not discussed here.

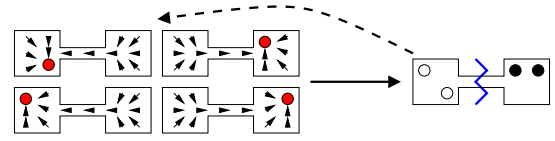


Figure 7: Influence-based model decomposition: sample an influence graph, and cluster probes and partition field based on similar control effects. Ambiguity-directed sampling techniques close the loop by suggesting new probe locations.

#### Field node equivalence predicate

Return true if nodes have similar-enough effect to one probe, false if they don't, and ambiguous if the magnitude of the effect is not large enough or if two competing probes yield similar effects.

#### Sample objective function

Perform secondary aggregation and classification to find regions of ambiguities. For each ambiguous field node, measure how similar its flows are to other ambiguous field nodes in its region; choose the node with the best similarity to the most ambiguous nodes.

Table 3: Domain knowledge for ambiguity-directed sampling in influence-based model decomposition.

The quality of decompositions from a small number of randomly-placed probes is competitive with that of a spectral partition of the complete influence graph (computed following an approach developed for image segmentation [Shi and Malik, 1997]), but with orders of magnitude less computation and in a decentralized model [Bailey-Kellogg and Zhao, 1999]. We now extend this approach to show that replacing random sampling with ambiguity-directed sampling achieves even better results. Ambiguity-directed sampling effectively closes the loop between the field decomposition and influence graph sampling (dashed arrow in Fig. 7). Tab. 3 describes the the domain-specific knowledge used in ambiguity-directed sampling for model-based decomposition.

We applied ambiguity-directed sampling to the three problems presented by [Bailey-Kellogg and Zhao, 1999]: a plus-shaped piece of material, a P-shaped piece of material, and an anisotropic bar, illustrating different geometries, topologies (the P-shaped material has a hole), and material properties. Results were collected for 1000 runs each by random probing, and using each possible node in the discretization for the initial probe in ambiguity-directed probing. Results are relative to a baseline spectral partitioning of the complete influence graph (computed essentially using probes at every one of the hundreds of nodes in a discretization).

Given a decomposition, a quality metric compares the amount of influence that stays within a region to the amount that leaves it: To be more specific, define the decomposition quality  $q$  ( $0 \leq q \leq 1$ ) for a partition  $P$  of a set of nodes  $S$  as follows ( $i$  is the influence):

$$q = \prod_{R \in P} \sum_{c \in R} \frac{\sum_{r \in R} i(c, r)}{\sum_{s \in S} i(c, s)}$$

Fig. 8 summarizes the results. The ambiguity-directed method generally does much better than random for a given

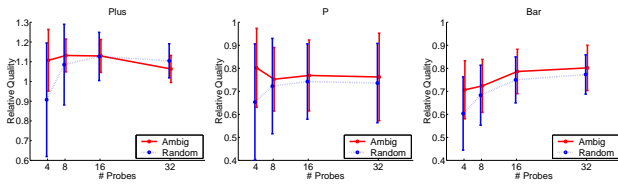


Figure 8: Comparison of influence-based model decomposition quality using random and ambiguity-directed probes, for three different problems: (left) plus; (middle) p; (right) bar. Results are relative to spectral partitioning.

number of probes, both in mean and standard deviation of quality, and it generally can do as well with 4-8 probes as random sampling can with 16-32. One interesting case is the taper in the plus-shaped piece of material. This is due to over-sampling: the samples are clustered in the middle of the plus, yielding a jagged decomposition that results in a worse quality score. In fact, with default parameters, the ambiguity-based metric declines to add samples beyond about 10, indicating that the field was adequately sampled. In order to achieve the desired number of samples, parameters were set to force sampling for only small information gain.

## 5 Discussion

The idea of selective sampling to satisfy particular design criteria arises in many contexts, such as Gaussian quadrature, spline smoothing in geometric design, remote sensing data acquisition, crystallography [Gopalakrishnan *et al.*, 2000] and engineering design optimization. In data mining, sampling has been viewed as a methodology to avoid costly disk accesses (this thread of research, however, doesn't address the issue of where to sample) [Kivinen and Mannila, 1994]. All these approaches (including ours) rely on capturing properties of a desirable design in terms of a novel objective function. The distinguishing feature of our work is that it uses *spatial* information gleaned from a higher level of abstraction to focus data collection at the field/simulation code layer. While flavors of the *consistent labeling* problem in mobile vision have this feature, they are more attuned to transferring information across two *successive* abstraction levels. The applications presented here are novel in that they span and connect arbitrary levels of abstraction, thus suggesting new ways to integrate qualitative and quantitative simulation [Berleant and Kuipers, 1998].

The effectiveness of our approach relies on the trustworthiness of the ambiguity detection mechanism and the ability to act decisively on new information. In both our applications, this was easily achieved by relying on fairly specific qualitative features whose causes are well understood. However, in other applications (e.g. phase portrait exploration for sensitivity analysis of highly non-normal matrices), it is difficult to distinguish between qualitative changes in problem characteristic and numerical error such as roundoff. In such cases, a more detailed modeling of qualitative behavior should be exploited for ambiguity-directed sampling to be successful. In terms of the pocket study, this might require a domain-specific enumeration of the various ways in which pockets

(and ambiguities in detecting them) can arise, and a probabilistic model of the elements of a SAL hierarchy using, say, superpositions of Bayesian expectation-maximization terms.

We plan to extend ambiguity-directed sampling into a completely probabilistic framework. We would like to be able to incorporate information from multiple, perhaps conflicting, SAL hierarchies. This is an emerging frontier in several applications (such as bioinformatics), where diverse experimental methodologies can cause contradictory results at the highest levels of abstraction. Our work provides some of the first encouraging results addressing such grand-challenge problems.

## 6 Acknowledgments

Thanks to Layne T. Watson (Virginia Tech) and Feng Zhao (Xerox PARC) for helpful discussions. This work is supported in part by the following grants to Bruce Randall Donald: National Science Foundation grants NSF IIS-9906790, NSF EIA-9901407, NSF EIA-9802068, NSF CDA-9726389, NSF EIA-9818299, NSF CISE/CDA-9805548, NSF IRI-9896020, and NSF IRI-9530785, U. S. Department of Justice contract 2000-DT-CX-K001, and an equipment grant from Microsoft Research; and NSF grant EIA-9984317 to Naren Ramakrishnan.

## References

- [Bailey-Kellogg and Zhao, 1999] C. Bailey-Kellogg and F. Zhao. Influence-based model decomposition. In *Proc. AAAI*, 1999.
- [Bailey-Kellogg *et al.*, 1996] C. Bailey-Kellogg, F. Zhao, and K. Yip. Spatial aggregation: language and applications. In *Proc. AAAI*, 1996.
- [Berleant and Kuipers, 1998] D. Berleant and B. Kuipers. Qualitative and quantitative simulation: bridging the gap. *Artificial Intelligence*, 95(2):215–255, 1998.
- [Boyan and Moore, 2000] J.A. Boyan and A.W. Moore. Learning evaluation functions to improve optimization by local search. *J. Machine Learning Research*, 1:77–112, 2000.
- [Gopalakrishnan *et al.*, 2000] V. Gopalakrishnan, B.G. Buchanan, and J.M. Rosenberg. Intelligent aids for parallel experiment planning and macromolecular crystallization. In *Proc. ISMB*, volume 8, pages 171–182, 2000.
- [Journel, 1986] A. Journel. Constrained Interpolation and Qualitative Information - The Soft Kriging Approach. *Mathematical Geology*, 18(2):269–286, November 1986.
- [Kivinen and Mannila, 1994] J. Kivinen and H. Mannila. The use of sampling in knowledge discovery. In *Proc. 13th ACM Symposium on Principles of Database Systems*, pages 77–85, 1994.
- [Knill *et al.*, 1999] D.L. Knill, A.A. Giunta, C.A. Baker, B. Grossman, W.H. Mason, R.T. Haftka, and L.T. Watson. Response Surface Models Combining Linear and Euler Aerodynamics for Supersonic Transport Design. *J. of Aircraft*, 36(1):75–86, 1999.
- [Ordóñez and Zhao, 2000] I. Ordóñez and F. Zhao. STA: Spatio-temporal aggregation with applications to analysis of diffusion-reaction phenomena. In *Proc. AAAI*, 2000.
- [Rice, 1992] J.R. Rice. Learning, Teaching, Optimization and Approximation. In E.N. Houstis, J.R. Rice, and R. Vichnevetsky, editors, *Expert Systems for Scientific Computing*, pages 89–123. North-Holland, Amsterdam, 1992.

- [Sacks *et al.*, 1989] J. Sacks, W.J. Welch, T.J. Mitchell, and H.P. Wynn. Design and Analysis of Computer Experiments. *Statistical Science*, 4(4):409–435, 1989.
- [Shi and Malik, 1997] J. Shi and J. Malik. Normalized cuts and image segmentation. In *Proc. CVPR*, 1997.
- [Witkin and Heckbert, 1994] A. Witkin and P. Heckbert. Using particles to sample and control implicit surfaces. In *Proc. SIGGRAPH*, 1994.
- [Yip and Zhao, 1996] K.M. Yip and F. Zhao. Spatial aggregation: theory and applications. *J. Artificial Intelligence Research*, 5, 1996.
- [Yip, 1991] K.M. Yip. *KAM: A system for intelligently guiding numerical experimentation by computer*. MIT Press, 1991.